



Discovery, synthesis and biological evaluation of 2-(4-(*N*-phenethylsulfamoyl)phenoxy)acetamides (SAPAs) as novel sphingomyelin synthase 1 inhibitors

Ya-li Li^a, Xiang-yu Qi^a, Hui Jiang^b, Xiao-dong Deng^a, Yan-ping Dong^d, Ting-bo Ding^a, Lu Zhou^a, Peng Men^a, Yong Chu^a, Ren-xiao Wang^{c,*}, Xian-cheng Jiang^{a,b,*}, De-yong Ye^{a,*}

^a Department of Medicinal Chemistry, School of Pharmacy, Fudan University, No. 826, Zhangheng Rd., Shanghai 201203, China

^b State University of New York Downstate Medical Center, Brooklyn, NY 11203, USA

^c State Key Lab of Bio-organic and Natural Products Chemistry, Shanghai Institute of Organic Chemistry, Chinese Academy of Sciences, Shanghai 200032, China

^d Department of Food and Pharmaceutical Engineering, Suihua University, Suihua 152061, China

ARTICLE INFO

Article history:

Received 26 June 2015

Revised 26 July 2015

Accepted 27 July 2015

Available online 30 July 2015

Keywords:

Sphingomyelin synthase

Inhibitor

Structure-based virtual screening

Molecular docking

Point mutagenesis

ABSTRACT

Sphingomyelin synthase (SMS) has been proved to be a potential drug target for the treatment of atherosclerosis. However, few SMS inhibitors have been reported. In this paper, structure-based virtual screening was performed on hSMS1. SAPA **1a** was discovered as a novel SMS1 inhibitor with an IC₅₀ value of 5.2 μM in enzymatic assay. A series of 2-(4-(*N*-phenethylsulfamoyl)phenoxy)acetamides (SAPAs) were synthesized and their biological activities toward SMS1 were evaluated. Among them, SAPA **1j** was found to be the most potent SMS1 inhibitor with an IC₅₀ value of 2.1 μM in vitro assay. The molecular docking studies suggested the interaction modes of SMS1 inhibitors and PC with the active site of SMS1. Site-directed mutagenesis validated the involvement of residues Arg342 and Tyr338 in enzymatic sphingomyelin production. The discovery of SAPA derivatives as a novel class of SMS1 inhibitors would advance the development of more effective SMS1 inhibitors.

© 2015 Elsevier Ltd. All rights reserved.

1. Introduction

Sphingomyelin (SM) is the most abundant sphingolipid in plasma membrane. It also accounts for approximately 20 percent of the phospholipids in human plasma, but 63–75 percent of plasma SM exists in atherogenic low density lipoprotein (LDL) and very low density lipoprotein (VLDL).^{1,2} Epidemic investigations have revealed that patients with type II hyperlipidemia have increased plasma SM levels and increased proportions of SM in

polar lipoprotein lipids.³ Furthermore, plasma SM level has been proved as an independent risk factor for coronary artery disease in humans.^{4,5}

Sphingomyelin synthase (SMS) is the last enzyme in SM biosynthetic pathway. It transfers the phosphocholine head group of phosphatidylcholine (PC) onto ceramide and thus releases SM and diacylglycerol (DAG).⁶ As a SMS isoform, SMS1 was expressed ubiquitously in all the tested tissues. However, SMS1 is the major SMS in macrophages. SMS1 is primarily localized to the *trans* Golgi^{7,8}, and is a key factor in the control of SM level in the cells and on the cell plasma membrane.^{6,9} Over-expression of SMS1 significantly increased the level of intracellular SM, atherogenic potential and subsequent atherosclerotic lesions in mice.^{10,11} Contrarily, SMS1 deficiency could reduce plasma and cell membrane SM levels and attenuate atherogenesis in mice.^{12,13} Thus SMS1 might serve as a potential therapeutic target of atherosclerosis. SMS1 inhibitors would be potent drugs for the treatment of atherosclerosis.¹⁴

There has been no report of SMS1 purified in its active form so far. However, human SMS1 has been cloned more than ten years ago.^{15,16} SMS1 has an N-terminal Sterile Alpha Motif (SAM) which has been proved to have no effect on SMS activity.^{7,17} Except the

Abbreviations: SM, sphingomyelin; SMS, sphingomyelin synthase; PC, phosphatidylcholine; DAG, diacylglycerol; TM, transmembrane; hSMS1, human sphingomyelin synthase 1; His, histidine; Asp, aspartic acid; SAPA, 2-(4-(*N*-phenethylsulfamoyl)phenoxy)acetamide; SAR, structure–activity relationships; Phe, phenylalanine; Leu, leucine; Ala, alanine; Arg, arginine; Trp, tryptophane; Tyr, tyrosine; C6-NBD-Cer, 6-((*N*-(7-nitrobenz-2-oxa-1,3-diazol-4-yl)amino)hexanoyl)-sphingosine; DMPC, 1,2-dimyristoyl-*sn*-glycero-3-phosphocholine; C6-NBD-SM, *N*-(*N*-(7-nitro-2,1,3-benzoxadiazol-4-yl)-epsilon-aminohexanoyl)sphingosyl phosphoryl choline; HPLC, high performance liquid chromatography; IC₅₀, 50% inhibitory concentration.

* Corresponding authors. Tel.: +86 21 54925128 (R.W.); tel.: +1 718 270 6701 (X.J.); tel./fax: +86 21 51980125 (D.Y.).

E-mail addresses: wangrx@mail.sioc.ac.cn (R.-x. Wang), xjiang@downstate.edu (X.-c. Jiang), dyye@shmu.edu.cn (D.-y. Ye).

SAM domain, the six transmembrane (TM1–TM6) and four highly conserved motifs (D1–D4) of *hSMS1* reside on the sequence of M130–Q353 amino acids.^{15,16} Two conserved motifs D3 (C277–T286 aa) and D4 (H328–H348 aa) localize at TM4 and TM6, respectively. Especially, motif D4 (H328–H348 aa) at TM6 is critical for the catalytic function of SMS1.¹⁸ For the discovery of SMS1 inhibitor, a three-dimensional structure of human sphingomyelin synthase 1 (*hSMS1*, M130–Q353 aa) has been built by homology modeling, optimized through molecular dynamics and proved the rationality.¹⁹ Moreover, a domain locating on motifs D3 and D4 of *hSMS1* was discovered to be the active site for SM production.¹⁵ Three residues His285, His328 and Asp332 in motifs D3 and D4, forming a HHD triad, have been proved to be key amino acids involved in SM production by site-directed mutagenesis.¹⁷ However, the roles of other amino acids in the active site as well as the catalytic mechanism involved in SM production were still under investigation.

Up to now, very few SMS inhibitors have been reported in the literatures. Potassium tricyclo[5.2.1.0(2,6)]-decan-8-yl-dithiocarbonate **D609** (Fig. 1), which was firstly found as a cytotoxic anti-virus and anti-tumor reagent,^{20,21} was reported with a weak SMS inhibitory effect in numerous enzyme or cell types in vitro (IC_{50} = 177–600 μ M).^{6,22–24} But the highly instable structure of **D609** ($t_{1/2}$ = 19.5 min in saline solution at 24 °C) hindered its further development to become an effective SMS inhibitor. Although the prodrug modification of **D609** could improve its chemical stability,²³ the inhibitory activity toward SMS should be enhanced. Furthermore, α -aminonitrile derivatives have been identified as the first series of SMS inhibitors discovered through rational design. Among them, the representative compound **D2** (Fig. 1) exhibited more potent SMS inhibitory activity than **D609**.^{25,26} However, the molecule of compound **D2** contains α -aminonitrile group, which is regarded as a potential toxicogenic structure. Therefore, more effective SMS1 inhibitors should be discovered to understand the role of SMS1 in cell functions and animal phenotypes as well as to meet the further study of SMS1 inhibitors as potent therapeutical drugs for the treatment of atherosclerosis.

In this study, structure-based virtual screening was performed to discover novel SMS1 inhibitors. A series of SAPA derivatives were designed and synthesized through structure sectionalized modification for in vitro enzymatic assay and SAR studies. Fortunately, six of them showed potent SMS1 inhibitory activities with IC_{50} values lower than 10 μ M in enzymatic assay. The binding modes of SMS1 inhibitors and substrate PC with *hSMS1* were investigated. The involvement of residues Arg342 and Tyr338 at the active site of *hSMS1* in SM production were evaluated by site-directed mutagenesis.

2. Results and discussion

2.1. Structure-based virtual screening of the SPECS library

A multi-step structure-based virtual screening was employed to discover potential small molecule SMS1 inhibitors. The SPECS

library (<http://www.specs.net>) was updated and contained over 220,000 compounds which were to be screened through molecular docking. The reported structural model of *hSMS1*¹⁹ was energy optimized before being employed in the virtual screening. The molecular docking was conducted by targeting the validated active site of *hSMS1* and performed on the GOLD software and the GLIDE software sequentially. A total of 95 compounds were finally selected among the top-ranked candidates after visual examination. The screening procedure was fully detailed in Section 4.

Samples of these 95 compounds were purchased from SPECS Inc and tested for their biological activities without further purification. The SMS1 inhibitory activities of these compounds were evaluated in an in vitro enzymatic assay. Among them, 2-(4-(*N*-phenethylsulfamoyl)phenoxy)acetamide (SAPA) derivative **1a** (Fig. 2), the only active compound, exhibited dose-dependent inhibition toward SMS1 overexpressed HeLa cell lysate with an IC_{50} value of 5.2 μ M (Fig. 3a). It was approximately forty fold more potent than **D609** which showed modest SMS1 inhibitory activity with an IC_{50} value of 219 μ M (Fig. 3b). Therefore SAPA **1a**, as a novel scaffold of SMS1 inhibitors, was considered to be the lead compound for further structural modification.

2.2. Chemistry

SAPA derivatives were designed and synthesized following the general route described in Scheme 1. The *N*-substituted-2-chloroacetamides **3a–3r** were synthesized by the nucleophilic substitution reaction of various substituted aniline or benzylamine **2a–2r** with chloroacetyl chloride in the presence of pyridine. Besides the key intermediate, 4-hydroxybenzene-1-sulfonyl chloride **5** was obtained from chloroformylation of compound **4** by thionyl chloride with catalytic amount of DMF. Then compounds **7a–7d** were prepared by the reaction of the intermediate **5** with different amines **6a–6d** in moderate yields after recrystallization. Finally the target compounds SAPA **1a** and **1d–1w** were achieved through the general electrophilic substitution of compounds **7a–7d** by 2-chloroacetamides **3a–3r**. The yields were in the range of 30–80% and the unfavorable attacking of nitrogen atom on sulfonamide group could be avoided by controlling temperature and ratio of substrates.

In order to investigate the role of sulfonyl group on **1a**, SAPA analogues **1b** and **1c** were designed and synthesized following the route described in Scheme 2. 4-Hydroxybenzoic acid **8** was treated with thionyl chloride in methanol under reflux condition to afford the corresponding methyl ester **9**. Then the intermediate **10** was afforded by the reaction of compound **9** with *N*-substituted-2-chloroacetamides **3a**. Subsequently the hydrolysis of compound **10** was carried out to give compound **11**, which was treated respectively with amines **6a** and **6e** to afford the corresponding SAPA analogues **1b** and **1c**.

The structures of all new compounds were elucidated from their analytical and spectroscopic data which were collected in the Section 4.

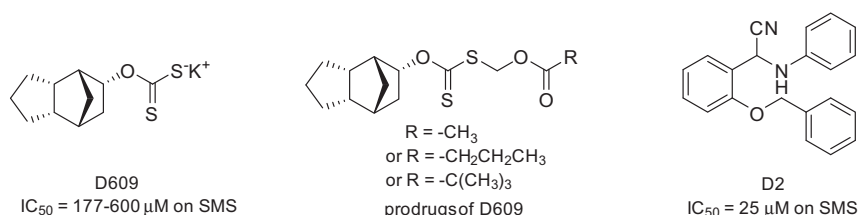


Figure 1. Chemical structures of reported sphingomyelin synthase inhibitors.

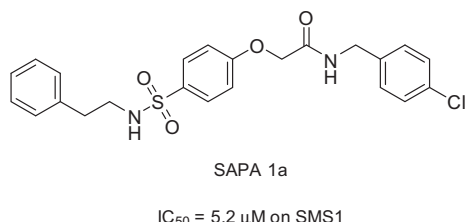


Figure 2. The chemical structure and SMS1 inhibitory activity of SAPA 1a.

2.3. Biological evaluation

All the newly prepared SAPA derivatives were evaluated for their SMS1 inhibitory activities with the publicly known inhibitor **D609** as the positive control. SMS1 overexpressed Hela cell lysate was prepared according to a method described in Section 4. The Hela cell lysate was pre-incubated with the corresponding SAPA derivatives at 37 °C for 30 min in the presence of test buffer. C6-NBD-Cer and DMPC were added as substrates into the biological test system. After the mixture was incubated at 37 °C for an additional 2 h, the resulting mixture was quenched and centrifuged. The amount of C6-NBD-Cer and C6-NBD-SM in the supernatant liquid were quantified by the fluorescent HPLC-based analysis.²⁷ Finally, the inhibitory activities of SAPA derivatives were evaluated by the decrease of the product C6-NBD-SM compared with control groups. The SMS1 inhibitory activities of SAPA derivatives were showed in Table 1. The IC_{50} values represent the compound concentration at which 50 percent of SMS1 activity was inhibited.

The results of biological evaluation exhibited that half of the SAPA derivatives could inhibit SMS1 activity with IC_{50} values lower than 25 μM . Among them, SAPA 1a, 1i, 1j, 1k, 1n and 1v showed potent SMS1 inhibitory activities with IC_{50} values lower than 10 μM . The SMS1 inhibitory activities of SAPA 1j, 1k, 1n and 1v were shown in Figure 4a–d respectively. Especially, SAPA 1j with the IC_{50} value of 2.1 μM on SMS1 inhibition was approximately one hundred fold more potent than **D609**. Therefore, SAPA 1j became the most potent SMS1 inhibitor to the best of our knowledge.

2.4. Structure–activity relationships (SAR) study

In order to explore the interesting enzymatic profile, a preliminary structure–activity relationship of SAPA derivatives was analyzed based on the results of in vitro SMS1 enzymatic assays.

Firstly, the substitution of sulfonyl group ($-SO_2-$, 1a) by carbonyl group ($-C=O-$, 1b) in SAPA derivatives could eliminate SMS1 inhibitory activities remarkably. It was indicated that the carbonyl group would diminish the interaction of SMS1 with sulfonyl group which might be vital for SMS1 inhibition. However, it should also be noticed that the sulfonyl group would not be the sole contributor to the SMS1 inhibitory activities of SAPA derivatives. The optimal size of chain between the sulfonamide ($-SO_2NH-$) with hydrophobic G group (1a vs 1d–1f) would also be necessary for SMS1 inhibitory activities. Moreover, SMS1 inhibitory activity was dramatically attenuated by the two methylene chain linking A ring with the amide ($-CONH-$, 1g vs 1h). It suggested that compound with longer chain linking A ring with the amide would not be accommodated by the limited domain of SMS1. Furthermore, the substituent R group attached to the A ring was also important for maintaining SMS1 inhibitory activities of SAPA derivatives. Both the steric and electronic effect of R group could contribute to the inhibitory activities of SAPA derivatives against SMS1. The introducing of substituent R group on para position of A ring (1h vs 1j) would be favorable for improving the inhibitory activity when the A ring was linked with the amide ($-CONH-$) by a methylene chain.

The structure–activity relationships achieved by SAPA derivatives would be helpful for developing more potent SMS1 inhibitors.

2.5. Molecular docking study

Molecular docking study was firstly performed using the GOLD software to investigate the interaction of SMS1 inhibitors with hSMS1. The binding mode of SAPA 1a with hSMS1 was showed in Figure 5a and b. As it was shown, SAPA 1a located at the active site of hSMS1 which was responsible for SM production and thus blocked the entry of PC as a substrate molecule. The segment of the amide ($-CONH-$) with 4-chlorobenzyl group of SAPA 1a reached into the interior of the domain where His285, His328 and Asp332 formed a triad, and was enveloped by hydrophobic residues Phe173, Phe177, Leu281 and Ala325. Meanwhile, the

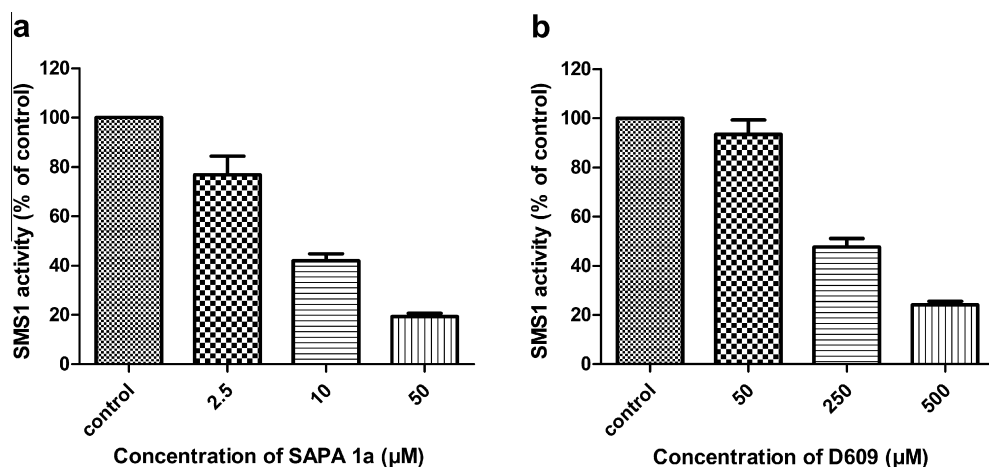
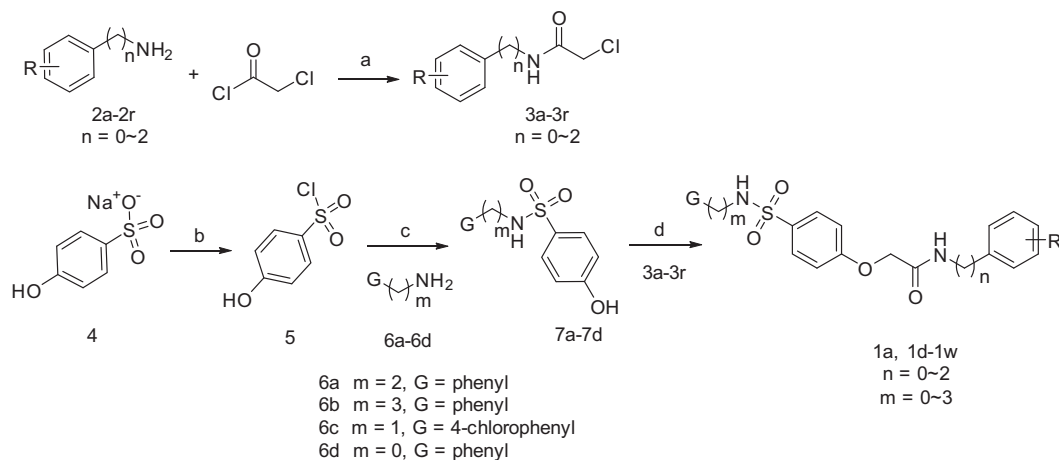
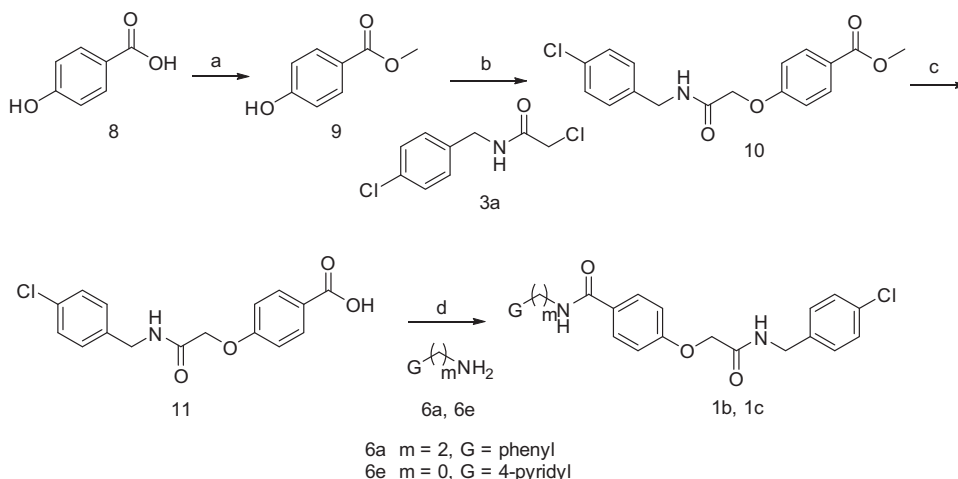


Figure 3. The SMS1 inhibitory activities of SAPA 1a and **D609**. The dose-dependent inhibition by three concentrations of SAPA 1a (2.5, 10 and 50 μM , respectively) against SMS1 is shown in Figure 3a. The modest inhibition by three concentrations of **D609** (50, 250 and 500 μM , respectively) against SMS1 is shown in Figure 3b. The results are expressed as percent of SMS1 activity in control groups in which there is no SMS1 inhibitor. The shown values are the means of triplicate assays. Values are shown in means \pm SD.



Scheme 1. General synthesis route for SAPA derivatives **1a** and **1d-1w**. Reagents and conditions: (a) H₂O/pyridine; (b) SOCl₂, DMF; (c) CH₂Cl₂, pyridine; (d) K₂CO₃, KI, acetone, 60 °C.



Scheme 2. Synthesis route for SAPA analogues **1b** and **1c**. Reagents and conditions: (a) SOCl₂, CH₃OH; (b) K₂CO₃, CH₃CN; (c) LiOH, H₂O/THF; (d) EDCI/HOBt, CH₂Cl₂.

sulfonamide (—SO₂NH—) group on SAPA **1a** interacted with residue Arg342 in motif D4 by forming hydrogen bond (2.4 Å) which would fix SAPA **1a** into the binding pocket. The unique interactions with residue Arg342 of *h*SMS1 were not detected in the reported binding mode of compound **D2** with *h*SMS1.²⁵ Furthermore, a π – π interaction was found between the middle benzene ring of SAPA **1a** and the imidazole ring of residue His285. Finally, the phenylethylamino group connecting with sulfonyl group lay fitly at a hydrophobic site encircled by residues Leu289 and Trp346.

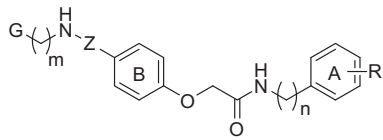
The binding mode of **D609** with *h*SMS1 was also illustrated (Fig. 5c and d) and compared with the mode of SAPA **1a** with *h*SMS1. As it was reported, the negative charged sulfur atom on **D609** formed a strong salt-bridge interaction with residue Arg342 under the support of residue Tyr338 which partly mimicked the hydrogen bonds between SAPA **1a** and *h*SMS1. It should be noted that there is no interaction formed between **D609** with the interior of the active site as SAPA **1a** did. The weak interaction of **D609** with *h*SMS1 may be the reason that it was less effective than SAPA **1a** toward SMS1 inhibition.

The interaction of SAPA **1b** with *h*SMS1 was further studied and revealed in Figure 5e and f. As the mode of SAPA **1a** with *h*SMS1, SAPA **1b** located at the active site of *h*SMS1. The segment of the amide (—CONH—) with 4-chlorobenzyl group of SAPA **1b** reached into the interior of the domain. However, as shown in Figure 5e,

SAPA **1b** had no interaction with residue Arg342 in motif D4. The carbonyl group (—C=O—) of SAPA **1b** demolished the hydrogen bonds formed between the sulfonamide (—SO₂NH—) group of SAPA **1a** and Arg342. The π – π interaction was also weakened by a dihedral angle formed by the middle benzene ring of SAPA **1b** and the imidazole ring of residue His285. The disadvantageous conformation of SAPA **1b** in the active site of *h*SMS1 might account for its remarkable decrease in SMS1 inhibitory activity. It also reinforced the hypothesis that the interaction with residue Arg342 in motif D4 might be important for SAPA derivatives and **D609** to hold their SMS1 inhibitory activities.

Finally, the interaction of substrate PC with *h*SMS1 was explored and illustrated in Figure 5g and h. The phosphocholine head group of PC reached into the HHD triad (His285, His328 and Asp332) formed domain, and was surrounded by a hydrophobic patch encircled by residues Phe173, Phe177, Leu281 and Ala325. In addition, substrate PC interacted with residue Arg342 in motif D4 by forming two hydrogen bonds (1.7 Å and 2.1 Å) which were more effective than that of SAPA **1a** with residue Arg342. The hydrogen bond formed between PC and residue Arg342 with the help of residue Tyr338 as its partner was favorable for locking the conformation of PC to facilitate the catalytic reaction. The two carbon chain tails of PC lay in the groove on the surface of *h*SMS1 (Fig. 5h). It should be noticed that residue Arg342

Table 1
SMS1 inhibitory activities of SAPA derivatives **1a–1w**



Compound	Z	G	m	n	R	SMS1 IC ₅₀ ^a (μM)
1a	Sulfonyl	Phenyl	2	1	4-Cl	5.2
1b	Carbonyl	Phenyl	2	1	4-Cl	>100
1c	Carbonyl	Pyridin-4-yl	0	1	4-Cl	>100
1d	Sulfonyl	Phenyl	3	1	4-Cl	>100
1e	Sulfonyl	4-Chlorophenyl	1	1	4-Cl	>50
1f	Sulfonyl	Phenyl	0	1	4-Cl	>100
1g	Sulfonyl	Phenyl	2	2	-H	>50
1h	Sulfonyl	Phenyl	2	1	-H	23.1
1i	Sulfonyl	Phenyl	2	1	4-OCH ₃	5.9
1j	Sulfonyl	Phenyl	2	1	4-Br	2.1
1k	Sulfonyl	Phenyl	2	1	4-F	8.1
1l	Sulfonyl	Phenyl	2	1	3-F	15.6
1m	Sulfonyl	Phenyl	2	0	-H	14.7
1n	Sulfonyl	Phenyl	2	0	4-Cl	6.6
1o	Sulfonyl	Phenyl	2	0	4-F	10.5
1p	Sulfonyl	Phenyl	2	0	4-OCH ₃	>50
1q	Sulfonyl	Phenyl	2	0	2-OCH ₃	14.2
1r	Sulfonyl	Phenyl	2	0	2-CH ₃	>100
1s	Sulfonyl	Phenyl	2	0	2-NO ₂	>100
1t	Sulfonyl	Phenyl	2	0	2-CN	>100
1u	Sulfonyl	Phenyl	2	0	2-OCF ₃	>100
1v	Sulfonyl	Phenyl	2	0	3-OCH ₃	9.2
1w	Sulfonyl	Phenyl	2	0	2-OCH ₃ , 4-F	>100
D609						219 ^b

^a IC₅₀ values are the means of three separate determinations on SMS1 overexpressed Hela cell lysate and were determined by more than five concentrations of each inhibitor.

^b The compound **D609** was used as a positive control in the biological assay. Statistical calculation of IC₅₀ values was performed on GraphPad Prism 5.02 (GraphPad Software, Inc.).

was involved in the interaction of *h*SMS1 not only with SMS1 inhibitors but also with substrate PC. Meanwhile, the cooperation between residues Arg342 and Tyr338 on the same motif D4 including a hydrogen bond (1.9 Å) and π -cation interaction were also detected in the docking modes of *h*SMS1 with SMS1 inhibitors as well as substrate PC.

The docking studies could illuminate the SMS1 inhibitory activity and the SAR of SAPA derivatives. The predicted role of residue Arg342 in the binding of *h*SMS1 with substrate PC or SMS1 inhibitors as well as its interaction with Tyr338 aroused our curiosity to investigate the unclear function of these residues in the catalytic reaction of SM production by SMS1.

2.6. Point mutagenesis

According to the putative five-step catalytic mechanism involved in SM production, the initiation of the reaction is involved in the binding of a two-chain choline phospholipid PC to the active site. Subsequently, His328 and Asp332 act coordinately to mediate a nucleophilic attack on phosphomonoester bond.¹⁵ However, the catalytic triad, His285, His328 and Asp332, in the center of the enzyme, needs support of other amino acid residues.

To evaluate the role of residues Arg342 and Tyr338 which are in motif D4 and the active site of SMS1, we replaced them with alanine and prepared Y338A and R342A respectively, using site-directed mutagenesis approach. All the methods were performed and modified as the study published by Yeang et.al.¹⁷ As

shown in Figure 6, Y338A and R342A significantly reduced their SMS1 activity. Notably, these experimental results fit very well with a previous virtual mutation analysis showing that R342A or Y338A causes a significant loss of binding energy in comparison with wild type.¹⁹ The result indicated that both Arg342 and Tyr338 have an effect on the catalytic activity of SMS1 and thus affect the SM production. It should be noted that, unlike H285A, H328A and D332A, Y338A and R342A do not eliminate the SMS1 activities utterly. Therefore, Arg342 and Tyr338 might play supportive roles in the catalytic SM production. The involvement of residues Arg342 and Tyr338 in SM production was helpful for understanding the mysterious catalytic mechanism of the SM production and for guiding the design of SMS1 inhibitors.

3. Conclusion

In summary, we have discovered SAPA **1a** as a novel SMS1 inhibitor through structure-based virtual screening. Twenty three SAPA derivatives were synthesized and half of them exhibited more potent SMS1 inhibitory activity than **D609**. Among them, SAPA **1j** is the most potent SMS1 inhibitor (IC₅₀ = 2.1 μM). The interaction modes of SMS1 inhibitors with *h*SMS1 were disclosed through molecular docking studies. The involvement of residues Arg342 and Tyr338 in the catalytic SM production were evaluated through point mutagenesis for the first time. Our study would provide a foundation for the further study of SMS1 catalytic mechanism and for the development of more potent SMS1 inhibitors.

4. Experimental protocols

4.1. Structure-based virtual screening

A multi-step structure-based virtual screening was employed to discover potential small molecule SMS inhibitors. Firstly, the entire SPECS library (~220,000 compounds, from <http://www.specs.net>) was filtered by drug-likeness rules, which required qualified candidates to have molecular weight lower than 1000 daltons, number of hydrogen bond acceptors and donors between 2 and 10, number of non-hydrogen atoms between 9 and 50, and no more than 10 rotatable single bonds. In this step we selected out approximately 80,000 qualified molecules. Then, these molecules were docked into the active site of *h*SMS1 using the GOLD software suite (version 5.0, released by CCDC). The *h*SMS1 structure was kept fixed during the entire docking process. Key parameters used in this docking task were set as follows: Island number = 5; population size on each island = 100; total genetic algorithm operations = 30,000; mutation rate = 95%; crossover rate = 95%; migration rate = 10%; scoring function = ChemScore. Up to twenty binding poses were generated for each docked molecule. After this step, 20,000 molecules with the highest binding scores were selected out.

These molecules selected by GOLD were further screened by the Glide module implemented in the Schrödinger software (version 2008, released by the Schrödinger Inc.) at the 'extra-precision' (XP) mode. Default parameters were employed in molecular docking. The *h*SMS1 structure was also kept fixed during this process. Then, the top-ranked 4000 molecules were subjected to similarity analysis to remove structurally redundant ones. Similarity matrix based on molecular fingerprint ECFP4 was generated by using Pipeline Pilot (released by Accelrys Inc.). A total of 500 clusters were obtained based on the similarity matrix. The compound with the highest Glide binding score was selected from each cluster. These 500 compounds were visually examined to eliminate (i) those in unreasonable binding poses, and (ii) those containing undesired chemical moieties or not suitable for further chemical

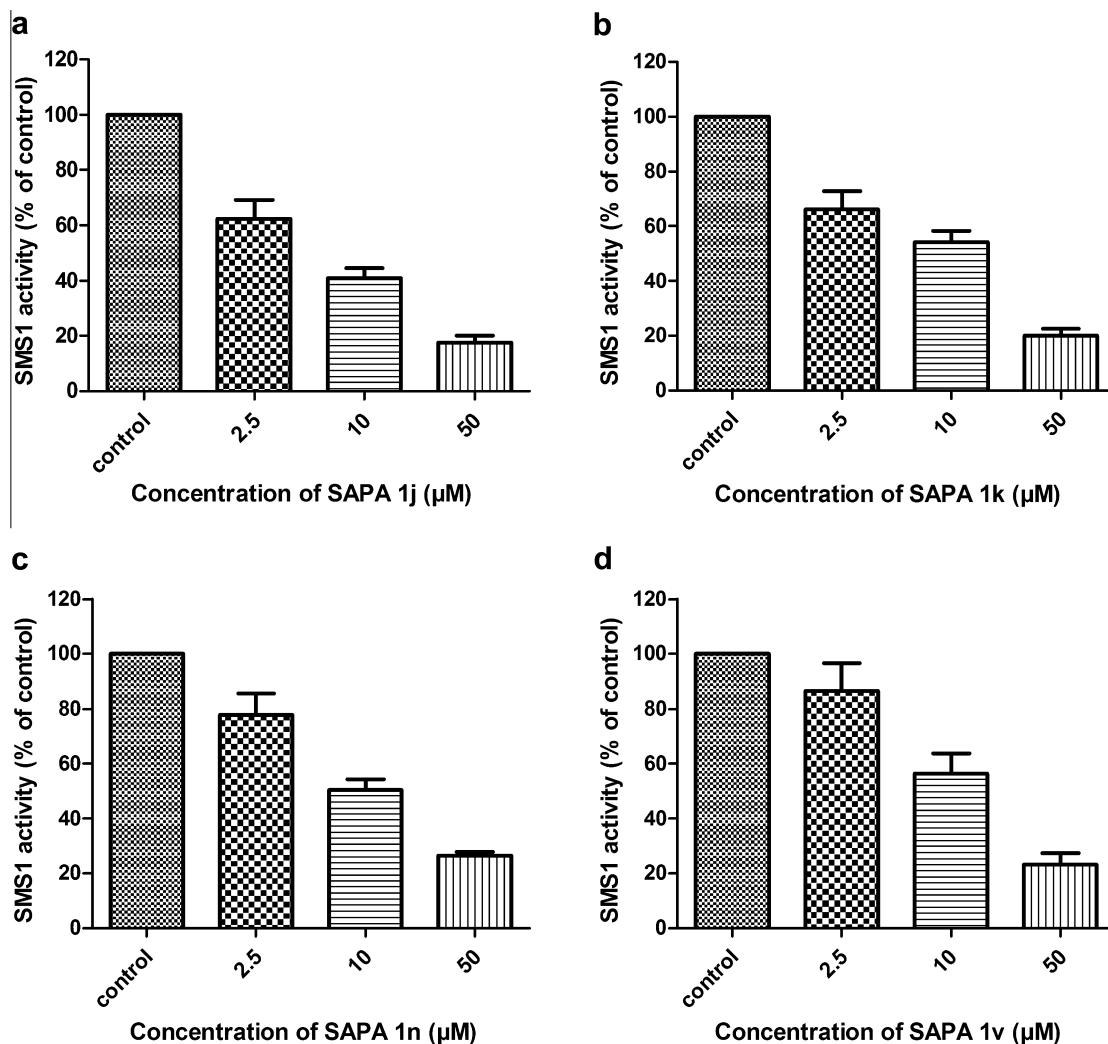


Figure 4. The SMS1 inhibitory activities of SAPA derivatives. The dose-dependent inhibition by different concentrations of SAPA **1j**, **1k**, **1n** and **1v** (2.5, 10 and 50 μM) against SMS1 are shown respectively in Figure 4a–d. The results are expressed as percent of SMS1 activity in control groups in which there is no SMS1 inhibitor. The shown values are the means of triplicate assays. Values are shown in means ± SD.

modification. Finally, a total of 95 compounds were selected as candidates. Samples of these compounds were purchased from the SPECS Inc. for subsequent biological evaluations.

4.2. Chemistry

Reagents were purchased from commercial sources and used without further purification except special case. Flash column chromatography was carried out at medium pressure using silica gel (200–300 mesh) purchased from Qingdao Haiyang Chemical Co. Ltd. All the reactions were monitored by thin layer chromatography (TLC) on silica gel. Mass spectra data were given with electro spray ionization (ESI) produced by a Finnigan MAT-95, LCQ-DECA spectrometer and IonSpec 4.7 T. MS. High resolution mass spectra data were given by AB 5600+ Q TOF. ^1H NMR and ^{13}C NMR spectra data were obtained on Varian Mercury Plus 400 spectrometers working at 400 MHz or Bruker Ascend™ 600 spectrometers working at 600 MHz. Chemical shifts (δ) were reported in parts per million (ppm) relative to internal tetramethylsilane (TMS) and J values were reported in Hertz. Peak multiplicity were described as singlet (s), doublet (d), triplet (t), quartet (q), multiplet (m), broad (br), broad singlet (br s), and broad multiplet (br m). The purities of all tested SAPA derivatives were higher than 95% by HPLC, which were performed on an Agilent 1260 HPLC system with a G1311B

quaternary pump, a G1329B ALS and a G4212B DAD detector. The HPLC method consisted of the following: Agilent C18 RP column (250 mm × 4.6 mm, 5 μm); column temperature 25 °C; inject volume 20 μl; HPLC solvent $\text{H}_2\text{O}/\text{CH}_3\text{OH}$ (0.1% TFA) = 30/70 (v/v); flow rate of 1.0 mL/min; detector wavelength of 254 nm. Retention times (t_R) were in minutes. Melting points were determined by a SGW X-4 thermometer and were uncorrected (slide method). The yield was not optimized.

4.2.1. The preparation of 2-(4-(*N*-phenethylsulfonyl)phenoxy)acetamides (SAPA **1a** and **1d–1w**)

4.2.1.1. 4-Hydroxybenzene-1-sulfonyl chloride (5). A mixture of sodium 4-hydroxybenzenesulfonate **4** (1.96 g, 10 mmol) in thionyl chloride (3.7 ml) and catalytic DMF (0.06 ml) was stirred at 60 °C for 3.5 h. After cooling to ambient temperature, the reaction mixture was poured into ice water (10 ml) and extracted by dichloromethane, washed with brine, dried over Na_2SO_4 . The organic solvent was evaporated and compound **5** was obtained as 1.93 g colorless oil. ESI-MS m/z 192.9 ($\text{M}+\text{H}$)⁺.

4.2.1.2. 4-Hydroxy-*N*-substituted-benzenesulfonamides (7a–7d). General procedure: To a solution of amine (10 mmol) in dichloromethane (20 ml) and pyridine (1.6 ml) was added the solution of 4-hydroxybenzene-1-sulfonyl chloride **5**

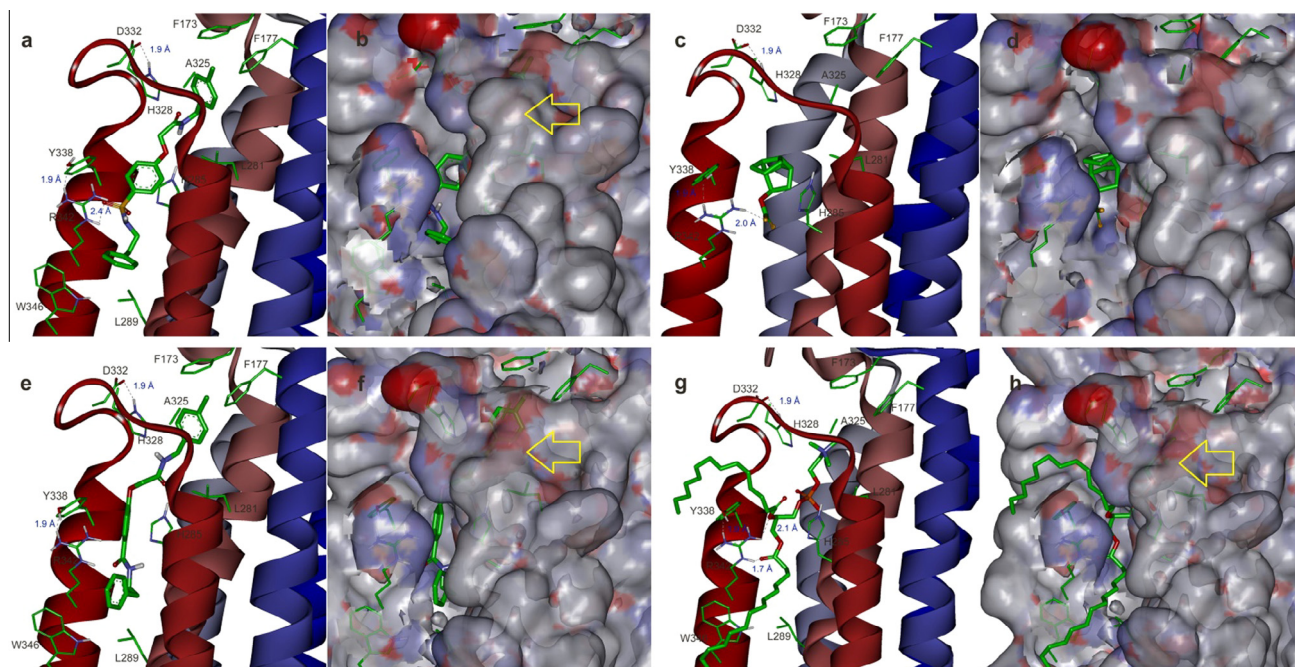


Figure 5. Docking studies of SMS1 inhibitors and PC at the active site of *hSMS1*. The docking studies were performed on the GOLD software suite (version 5.0, released by CCDC). The interaction of SAPA **1a**, **D609**, SAPA **1b** and substrate PC with *hSMS1* displayed by solid ribbons are shown in Figure 5a, c, e and g. The interaction of SAPA **1a**, **D609**, SAPA **1b** and substrate PC with *hSMS1* displayed the protein surface are shown respectively in Figure 5b, d, f and h. The ribbons in colors stand for the six transmembrane (TM1–TM6) of *hSMS1*. The active site of *hSMS1* composed of motifs D3 (C277–T286 aa) and D4 (H328–H348 aa) localizes at TM4 (ribbon in brownish red) and TM6 (ribbon in red) respectively. Black dashed lines stand for hydrogen bonds or salt bridges. The length of hydrogen bonds or salt bridges is shown by characters in blue with the unit Å. The protein surface of *hSMS1* is shown in electrostatic surface with transparency. The yellow arrows on the protein in Figure 5b, d, f and h point to the interior of *hSMS1* that SAPA **1a**, SAPA **1b** and substrate PC reached.

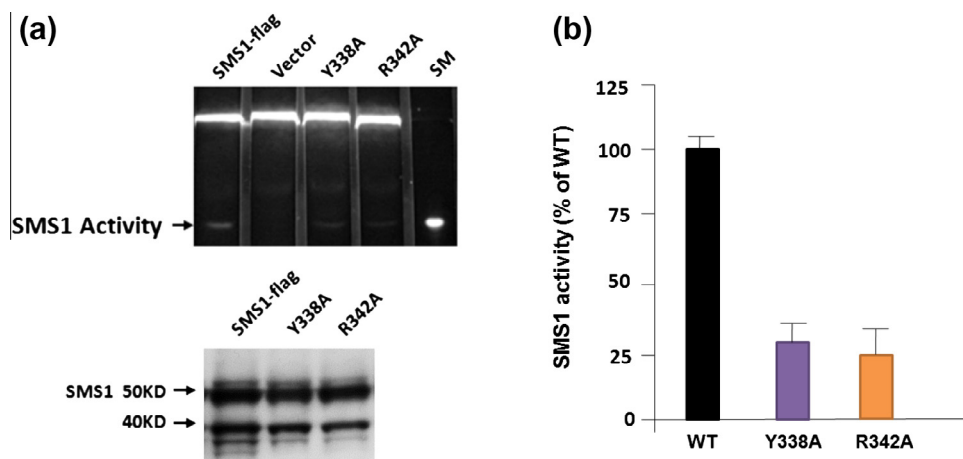


Figure 6. The activities and protein levels of wild type and point mutated SMS1. The SMS1 activities were performed on wild type (WT) or mutant SMS1 (Y338A and R342A) and results are shown in Figure 6a. The protein levels of each enzyme are shown in a western blot in Figure 6a. The quantitative comparison of wild type SMS1 (WT) with point mutated SMS1 (Y338A and R342A) on SMS1 activity is shown in Figure 6b. The shown values are the means of triplicate assays. Values are means \pm SD.

(1.93 g, 10 mmol) in dichloromethane (10 ml) slowly at 0 °C. The reaction mixture was stirred at room temperature for 1.5 h, washed with 1 mol/L HCl (aq) and brine, and then dried over Na_2SO_4 . After the organic solvent was evaporated, the crude product was recrystallized in dichloromethane and 4-hydroxy-*N*-substituted-benzenesulfonamide **7a–7d** were obtained as light yellow solid (two steps yield 30–40%). **7a** mp 137.1–139.8 °C. ESI-MS m/z 276.1 ($\text{M}-\text{H}^-$). ^1H NMR (400 MHz, $\text{DMSO}-d_6$) δ 10.37 (s, 1H), 7.61 (d, J = 8.6 Hz, 2H), 7.44 (t, J = 5.7 Hz, 1H), 7.26 (t, J = 7.3 Hz, 2H), 7.19 (d, J = 6.7 Hz, 1H), 7.14 (d, J = 7.4 Hz, 2H), 6.90 (d, J = 8.6 Hz, 2H), 2.90 (dd, J = 14.2, 6.7 Hz, 2H), 2.66 (t, J = 7.5 Hz, 2H). ^{13}C NMR (151 MHz, $\text{DMSO}-d_6$) δ 161.3, 139.3, 130.8, 129.3, 129.1, 128.8, 126.7, 116.0, 44.6, 35.7.

4.2.1.3. *N*-Substituted-2-chloroacetamides (3a–3r). General procedure: To a solution of aniline or benzylamine (10 mmol) in water (20 ml) and pyridine (1.6 ml) was added chloroacetyl chloride (1.69 g, 15 mmol) slowly at 0 °C. The reaction mixture was stirred at 0 °C for 1.0 h and then diluted with water (50 ml). The precipitate was collected by filtration, washed with water and dried under vacuum. *N*-substituted-2-chloroacetamides **3a–3r** were obtained as solid (yield 50–80%).

4.2.1.4. *N*-(4-Chlorobenzyl)-2-(4-(*N*-phenethylsulfamoyl)phenoxy)acetamide (SAPA **1a).** A mixture of 2-chloro-*N*-(4-chlorobenzyl)acetamide **3a** (0.22 g, 1.0 mmol), 4-hydroxy-*N*-phenethyl-benzenesulfonamide **7a** (0.42 g, 1.5 mmol), K_2CO_3 (0.21 g,

1.5 mmol) and KI (33 mg, 0.2 mmol) in acetone (20 ml) was stirred at 60 °C for 7.0 h. After the organic solvent was evaporated, the residual was diluted with water (20 ml), extracted with dichloromethane, washed with brine and then dried over Na₂SO₄. After filtration and condensation, the crude product was obtained and recrystallized in ethyl acetate/hexane (1:1, v: v) to afford **1a** as white solid (0.19 g, yield 42%); mp 151.4–153.3 °C. ESI-MS *m/z* 459.2 (M+H)⁺. HRMS (ESI) of C₂₃H₂₃ClN₂O₄S (M+H)⁺ calcd, 459.1140; found, 459.1145. ¹H NMR (400 MHz, DMSO-*d*₆) δ 8.74 (t, *J* = 6.1 Hz, 1H), 7.70 (d, *J* = 8.8 Hz, 2H), 7.58 (t, *J* = 5.5 Hz, 1H), 7.34 (d, *J* = 8.3 Hz, 2H), 7.24 (dd, *J* = 7.9, 6.1 Hz, 4H), 7.17 (d, *J* = 7.3 Hz, 1H), 7.11 (t, *J* = 7.9 Hz, 4H), 4.65 (s, 2H), 4.30 (d, *J* = 6.1 Hz, 2H), 2.89 (dd, *J* = 13.2, 7.1 Hz, 2H), 2.65 (t, *J* = 7.5 Hz, 2H). ¹³C NMR (101 MHz, DMSO-*d*₆) δ 167.2, 160.4, 138.6, 138.2, 132.6, 131.3, 129.0, 128.6, 128.3, 128.1, 126.2, 115.1, 66.9, 44.0, 41.1, 35.1. HPLC purity: *t*_R = 10.742, 98.5%.

4.2.1.5. N-(4-Chlorobenzyl)-2-(4-(N-(3-phenylpropyl)sulfamoyl)phenoxy)acetamide (SAPA 1d). SAPA **1d** was prepared by the reaction of **3a** with 4-hydroxy-*N*-(3-phenylpropyl)benzenesulfonamide **7b** according to the procedure described for SAPA **1a**. Yield 35%; mp 153.2–155.9 °C. ESI-MS *m/z* 473.3 (M+H)⁺. HRMS (ESI) of C₂₄H₂₅ClN₂O₄S (M+H)⁺ calcd, 473.1296; found, 473.1302. ¹H NMR (400 MHz, DMSO-*d*₆) δ 8.75 (s, 1H), 7.70 (d, *J* = 8.5 Hz, 2H), 7.52 (s, 1H), 7.35 (d, *J* = 8.0 Hz, 2H), 7.23 (dd, *J* = 12.7, 7.7 Hz, 4H), 7.18–7.06 (m, 5H), 4.66 (s, 2H), 4.32 (d, *J* = 5.5 Hz, 2H), 2.69 (d, *J* = 5.9 Hz, 2H), 2.52 (d, *J* = 7.6 Hz, 2H), 1.70–1.55 (m, 2H). ¹³C NMR (151 MHz, DMSO-*d*₆) δ 167.8, 160.9, 141.8, 138.8, 133.4, 131.8, 129.6, 129.0, 128.7, 128.6, 126.2, 115.6, 67.5, 42.5, 41.7, 32.6, 31.3. HPLC purity: *t*_R = 13.728, 98.5%.

4.2.1.6. N-(4-Chlorobenzyl)-2-(4-(N-(4-chlorobenzyl)sulfamoyl)phenoxy)acetamide (SAPA 1e). SAPA **1e** was prepared by the reaction of **3a** with *N*-(4-chlorobenzyl)-4-hydroxybenzenesulfonamide **7c** according to the procedure described for SAPA **1a**. Yield 41%; mp 144.2–146.0 °C. ESI-MS *m/z* 479.0 (M+H)⁺. HRMS (ESI) of C₂₂H₂₀Cl₂N₂O₄S (M+H)⁺ calcd, 479.0594; found, 479.0592. ¹H NMR (400 MHz, DMSO-*d*₆) δ 8.75 (s, 1H), 8.07 (s, 1H), 7.72 (d, *J* = 8.7 Hz, 2H), 7.39–7.29 (m, 4H), 7.25 (t, *J* = 8.5 Hz, 4H), 7.11 (d, *J* = 8.7 Hz, 2H), 4.66 (s, 2H), 4.32 (d, *J* = 5.9 Hz, 2H), 3.92 (d, *J* = 3.6 Hz, 2H). ¹³C NMR (151 MHz, DMSO-*d*₆) δ 167.8, 161.0, 138.8, 137.4, 133.5, 132.2, 131.9, 129.9, 129.6, 129.1, 128.6, 115.6, 67.5, 45.8, 41.7. HPLC purity: *t*_R = 12.924, 99.2%.

4.2.1.7. N-(4-Chlorobenzyl)-2-(4-(N-phenylsulfamoyl)phenoxy)acetamide (SAPA 1f). SAPA **1f** was prepared by the reaction of **3a** with 4-hydroxy-*N*-phenylbenzenesulfonamide **7d** according to the procedure described for SAPA **1a**. Yield 39%; mp 192.0–193.7 °C. ESI-MS *m/z* 431.1 (M+H)⁺. HRMS (ESI) of C₂₁H₁₉ClN₂O₄S (M+H)⁺ calcd, 431.0827; found, 431.0831. ¹H NMR (400 MHz, DMSO-*d*₆) δ 10.17 (s, 1H), 8.70 (s, 1H), 7.69 (d, *J* = 8.8 Hz, 2H), 7.32 (d, *J* = 8.3 Hz, 2H), 7.20 (dd, *J* = 12.2, 8.2 Hz, 4H), 7.10–7.03 (m, 4H), 6.99 (t, *J* = 7.3 Hz, 1H), 4.61 (s, 2H), 4.28 (d, *J* = 5.9 Hz, 2H). ¹³C NMR (151 MHz, DMSO-*d*₆) δ 167.7, 161.3, 138.7, 138.4, 132.4, 131.8, 129.6, 129.5, 129.3, 128.6, 124.3, 120.3, 115.6, 67.4, 41.6. HPLC purity: *t*_R = 7.806, 98.4%.

4.2.1.8. N-Phenethyl-2-(4-(N-phenethylsulfamoyl)phenoxy)acetamide (SAPA 1g). SAPA **1g** was prepared by the reaction of 2-chloro-*N*-phenethylacetamide **3b** with **7a** according to the procedure described for SAPA **1a**. Yield 37%; mp 127.6–129.8 °C. ESI-MS *m/z* 439.2 (M+H)⁺. HRMS (ESI) of C₂₄H₂₆N₂O₄S (M+H)⁺ calcd, 439.1686; found, 439.1690. ¹H NMR (400 MHz, DMSO-*d*₆) δ 8.22 (s, 1H), 7.69 (d, *J* = 8.8 Hz, 2H), 7.58 (t, *J* = 5.6 Hz, 1H), 7.29–7.21 (m, 4H), 7.17 (dd, *J* = 6.3, 4.3 Hz, 4H), 7.13 (d,

J = 7.1 Hz, 2H), 7.06 (d, *J* = 8.8 Hz, 2H), 4.55 (s, 2H), 3.35 (s, 2H), 2.90 (dd, *J* = 13.4, 7.1 Hz, 2H), 2.72 (t, *J* = 7.3 Hz, 2H), 2.65 (t, *J* = 7.5 Hz, 2H). ¹³C NMR (151 MHz, DMSO-*d*₆) δ 166.8, 160.4, 139.1, 138.6, 132.5, 128.5, 128.2, 126.1, 125.9, 114.9, 66.8, 43.9, 39.8, 35.1, 34.9. HPLC purity: *t*_R = 8.995, 98.0%.

4.2.1.9. N-Benzyl-2-(4-(N-phenethylsulfamoyl)phenoxy)acetamide (SAPA 1h). SAPA **1h** was prepared by the reaction of *N*-benzyl-2-chloroacetamide **3c** with **7a** according to the procedure described for SAPA **1a**. Yield 62%; mp 118.8–121.4 °C. ESI-MS *m/z* 425.2 (M+H)⁺. HRMS (ESI) of C₂₃H₂₄N₂O₄S (M+H)⁺ calcd, 425.1530; found, 425.1526. ¹H NMR (400 MHz, DMSO-*d*₆) δ 8.71 (t, *J* = 6.1 Hz, 1H), 7.75–7.69 (m, 2H), 7.58 (t, *J* = 5.8 Hz, 1H), 7.33–7.18 (m, 8H), 7.18–7.10 (m, 4H), 4.67 (s, 2H), 4.34 (d, *J* = 6.1 Hz, 2H), 2.96–2.88 (q, *J* = 7.5 Hz, 2H), 2.67 (t, *J* = 7.5 Hz, 2H). ¹³C NMR (101 MHz, DMSO-*d*₆) δ 167.1, 160.4, 139.1, 138.6, 132.5, 128.6, 128.5, 128.3, 128.2, 127.1, 126.7, 126.2, 115.0, 66.9, 44.0, 41.7, 35.2. HPLC purity: *t*_R = 7.358, 100%.

4.2.1.10. N-(4-Methoxybenzyl)-2-(4-(N-phenethylsulfamoyl)phenoxy)acetamide (SAPA 1i). SAPA **1i** was prepared by the reaction of 2-chloro-*N*-(4-methoxybenzyl)acetamide **3d** with **7a** according to the procedure described for SAPA **1a**. Yield 53%; mp 129.8–131.7 °C. ESI-MS *m/z* 455.2 (M+H)⁺. HRMS (ESI) of C₂₄H₂₆N₂O₅S (M+H)⁺ calcd, 455.1635; found, 455.1639. ¹H NMR (400 MHz, DMSO-*d*₆) δ 8.64 (t, *J* = 6.0 Hz, 1H), 7.70 (d, *J* = 8.8 Hz, 2H), 7.58 (t, *J* = 5.6 Hz, 1H), 7.25 (t, *J* = 7.3 Hz, 2H), 7.20–7.08 (m, 7H), 6.84 (d, *J* = 8.6 Hz, 2H), 4.62 (s, 2H), 4.25 (d, *J* = 6.0 Hz, 2H), 3.70 (s, 3H), 2.90 (q, *J* = 7.2 Hz, 2H), 2.65 (t, *J* = 7.5 Hz, 2H). ¹³C NMR (101 MHz, DMSO-*d*₆) δ 167.0, 160.5, 158.2, 138.7, 132.6, 131.1, 128.6, 128.3, 126.2, 115.1, 113.6, 66.9, 55.0, 44.1, 41.2, 35.2. HPLC purity: *t*_R = 7.059, 97.4%.

4.2.1.11. N-(4-Bromobenzyl)-2-(4-(N-phenethylsulfamoyl)phenoxy)acetamide (SAPA 1j). SAPA **1j** was prepared by the reaction of *N*-(4-bromobenzyl)-2-chloroacetamide **3e** with **7a** according to the procedure described for SAPA **1a**. Yield 60%; mp 152.6–154.7 °C. ESI-MS *m/z* 503.1 (M+H)⁺. HRMS (ESI) of C₂₃H₂₃BrN₂O₄S (M+H)⁺ calcd, 503.0635; found, 503.0639. ¹H NMR (400 MHz, DMSO-*d*₆) δ 8.74 (t, *J* = 5.8 Hz, 1H), 7.71 (d, *J* = 8.6 Hz, 2H), 7.58 (t, *J* = 5.7 Hz, 1H), 7.48 (d, *J* = 8.2 Hz, 2H), 7.25 (t, *J* = 7.3 Hz, 2H), 7.18 (d, *J* = 8.2 Hz, 3H), 7.12 (t, *J* = 8.2 Hz, 4H), 4.65 (s, 2H), 4.29 (d, *J* = 5.9 Hz, 2H), 2.90 (q, *J* = 13.7, 6.8 Hz, 2H), 2.65 (t, *J* = 7.5 Hz, 2H). ¹³C NMR (101 MHz, DMSO-*d*₆) δ 167.5, 160.6, 138.8, 132.8, 131.2, 129.6, 128.8, 128.5, 126.4, 120.0, 115.3, 67.1, 44.3, 41.4, 35.3. HPLC purity: *t*_R = 11.923, 98.7%.

4.2.1.12. N-(4-Fluorobenzyl)-2-(4-(N-phenethylsulfamoyl)phenoxy)acetamide (SAPA 1k). SAPA **1k** was prepared by the reaction of 2-chloro-*N*-(4-fluorobenzyl)acetamide **3f** with **7a** according to the procedure described for SAPA **1a**. Yield 61%; mp 148.0–150.6 °C. ESI-MS *m/z* 443.2 (M+H)⁺. HRMS (ESI) of C₂₃H₂₃FN₂O₄S (M+H)⁺ calcd, 443.1435; found, 443.1439. ¹H NMR (400 MHz, DMSO-*d*₆) δ 8.72 (t, *J* = 6.1 Hz, 1H), 7.70 (d, *J* = 8.8 Hz, 2H), 7.58 (t, *J* = 5.8 Hz, 1H), 7.29–7.21 (m, 4H), 7.18 (d, *J* = 7.2 Hz, 1H), 7.11 (m, *J* = 8.6, 4.3 Hz, 6H), 4.64 (s, 2H), 4.30 (d, *J* = 6.0 Hz, 2H), 2.90 (q, *J* = 7.2 Hz, 2H), 2.65 (t, *J* = 7.5 Hz, 2H). ¹³C NMR (101 MHz, DMSO-*d*₆) δ 167.2, 160.4, 138.7, 135.4, 132.6, 129.2, 128.6, 128.3, 126.2, 115.1, 115.0, 114.8, 66.9, 44.1, 41.1, 35.2. HPLC purity: *t*_R = 7.652, 98.2%.

4.2.1.13. N-(3-Fluorobenzyl)-2-(4-(N-phenethylsulfamoyl)phenoxy)acetamide (SAPA 1l). SAPA **1l** was prepared by the reaction of 2-chloro-*N*-(3-fluorobenzyl)acetamide **3g** with **7a** according to the procedure described for SAPA **1a**. Yield 52%; mp

139.4–141.6 °C. ESI-MS m/z 443.2 (M+H)⁺. HRMS (ESI) of C₂₃H₂₃-FN₂O₄S (M+H)⁺ calcd, 443.1435; found, 443.1440. ¹H NMR (400 MHz, DMSO-*d*₆) δ 8.76 (t, *J* = 5.9 Hz, 1H), 7.71 (d, *J* = 8.5 Hz, 2H), 7.58 (t, *J* = 5.8 Hz, 1H), 7.32 (dd, *J* = 13.9, 7.7 Hz, 1H), 7.25 (t, *J* = 7.1 Hz, 2H), 7.18 (d, *J* = 6.7 Hz, 1H), 7.12 (t, *J* = 6.7 Hz, 4H), 7.04 (dd, *J* = 17.6, 7.8 Hz, 3H), 4.67 (s, 2H), 4.34 (d, *J* = 5.7 Hz, 2H), 2.89 (q, *J* = 6.8 Hz, 2H), 2.65 (t, *J* = 7.3 Hz, 2H). ¹³C NMR (101 MHz, DMSO-*d*₆) δ 167.4, 163.4, 161.0, 160.5, 142.3, 142.2, 138.7, 132.6, 130.2, 128.7, 128.4, 126.3, 123.2, 115.1, 113.9, 113.7, 113.5, 66.9, 44.1, 41.3, 35.2. HPLC purity: *t*_R = 7.603, 98.2%.

4.2.1.14. 2-(4-(*N*-Phenethylsulfamoyl)phenoxy)-*N*-phenylacetamide (SAPA 1m). SAPA 1m was prepared by the reaction of 2-chloro-*N*-phenylacetamide 3h with 7a according to the procedure described for SAPA 1a. Yield 65%; mp 140.4–143.2 °C. ESI-MS m/z 411.2 (M+H)⁺. HRMS (ESI) of C₂₂H₂₂N₂O₄S (M+H)⁺ calcd, 411.1373; found, 411.1374. ¹H NMR (400 MHz, DMSO-*d*₆) δ 10.15 (s, 1H), 7.72 (d, *J* = 8.9 Hz, 2H), 7.61 (d, *J* = 7.7 Hz, 2H), 7.57 (t, *J* = 5.8 Hz, 1H), 7.31 (t, *J* = 7.9 Hz, 2H), 7.24 (t, *J* = 7.3 Hz, 2H), 7.20–7.10 (m, 5H), 7.07 (t, *J* = 7.4 Hz, 1H), 4.80 (s, 2H), 2.96–2.86 (q, *J* = 7.6 Hz, 2H), 2.65 (t, *J* = 7.5 Hz, 2H). ¹³C NMR (101 MHz, DMSO-*d*₆) δ 165.9, 160.6, 138.7, 138.3, 132.6, 128.7, 128.6, 128.3, 126.2, 123.7, 119.6, 115.0, 67.0, 44.1, 35.2. HPLC purity: *t*_R = 7.652, 100%.

4.2.1.15. *N*-(4-Chlorophenyl)-2-(4-(*N*-phenethylsulfamoyl)phenoxy)acetamide (SAPA 1n). SAPA 1n was prepared by the reaction of 2-chloro-*N*-(4-chlorophenyl)acetamide 3i with 7a according to the procedure described for SAPA 1a. Yield 68%; mp 179.8–181.6 °C. ESI-MS m/z 445.2 (M+H)⁺. HRMS (ESI) of C₂₂H₂₁-ClN₂O₄S (M+H)⁺ calcd, 445.0983; found, 445.0979. ¹H NMR (400 MHz, DMSO-*d*₆) δ 10.29 (s, 1H), 7.71 (d, *J* = 8.7 Hz, 2H), 7.65 (d, *J* = 8.7 Hz, 2H), 7.58 (t, *J* = 5.7 Hz, 1H), 7.37 (d, *J* = 8.8 Hz, 2H), 7.24 (t, *J* = 7.3 Hz, 2H), 7.17 (d, *J* = 7.1 Hz, 1H), 7.13 (dd, *J* = 7.6, 5.4 Hz, 4H), 4.81 (s, 2H), 2.91 (q, *J* = 7.0 Hz, 2H), 2.65 (t, *J* = 7.5 Hz, 2H). ¹³C NMR (101 MHz, DMSO-*d*₆) δ 166.2, 160.6, 138.7, 137.3, 132.7, 128.7, 128.3, 127.4, 126.3, 121.2, 115.1, 67.0, 44.1, 35.2. HPLC purity: *t*_R = 13.132, 99.1%.

4.2.1.16. *N*-(4-Fluorophenyl)-2-(4-(*N*-phenethylsulfamoyl)phenoxy)acetamide (SAPA 1o). SAPA 1o was prepared by the reaction of 2-chloro-*N*-(4-fluorophenyl)acetamide 3j with 7a according to the procedure described for SAPA 1a. Yield 61%; mp 137.6–139.7 °C. ESI-MS m/z 429.2 (M+H)⁺. HRMS (ESI) of C₂₂H₂₁-FN₂O₄S (M+H)⁺ calcd, 429.1279; found, 429.1283. ¹H NMR (400 MHz, DMSO-*d*₆) δ 10.20 (s, 1H), 7.71 (d, *J* = 8.7 Hz, 2H), 7.63 (dd, *J* = 8.7, 5.1 Hz, 2H), 7.57 (s, 1H), 7.24 (t, *J* = 7.3 Hz, 2H), 7.20–7.10 (m, 7H), 4.79 (s, 2H), 2.91 (d, *J* = 6.0 Hz, 2H), 2.64 (t, *J* = 7.4 Hz, 2H). ¹³C NMR (151 MHz, DMSO-*d*₆) δ 166.4, 161.1, 159.6, 158.0, 139.2, 135.1, 133.2, 129.1, 128.8, 126.7, 122.1, 115.9, 115.7, 115.5, 67.5, 44.5, 35.7. HPLC purity: *t*_R = 8.388, 100%.

4.2.1.17. *N*-(4-Methoxyphenyl)-2-(4-(*N*-phenethylsulfamoyl)phenoxy)acetamide (SAPA 1p). SAPA 1p was prepared by the reaction of 2-chloro-*N*-(4-methoxyphenyl)acetamide 3k with 7a according to the procedure described for SAPA 1a. Yield 79%; mp 172.7–174.4 °C. ESI-MS m/z 441.2 (M+H)⁺. HRMS (ESI) of C₂₃H₂₄N₂O₅S (M+H)⁺ calcd, 441.1479; found, 441.1478. ¹H NMR (400 MHz, DMSO-*d*₆) δ 10.00 (s, 1H), 7.71 (d, *J* = 8.7 Hz, 2H), 7.57 (t, *J* = 5.2 Hz, 1H), 7.51 (d, *J* = 8.9 Hz, 2H), 7.24 (t, *J* = 7.2 Hz, 2H), 7.17 (d, *J* = 7.3 Hz, 1H), 7.16–7.10 (m, 4H), 6.88 (d, *J* = 8.9 Hz, 2H), 4.76 (s, 2H), 3.70 (s, 3H), 2.91 (dd, *J* = 13.1, 6.9 Hz, 2H), 2.65 (t, *J* = 7.5 Hz, 2H). ¹³C NMR (151 MHz, DMSO-*d*₆) δ 166.0, 161.2, 156.1, 139.2, 133.2, 131.8, 129.1, 128.8, 126.7, 121.9, 115.5, 114.3, 67.6, 55.7, 44.6, 35.7. HPLC purity: *t*_R = 7.121, 100%.

4.2.1.18. *N*-(2-Methoxyphenyl)-2-(4-(*N*-phenethylsulfamoyl)phenoxy)acetamide (SAPA 1q). SAPA 1q was prepared by the reaction of 2-chloro-*N*-(2-methoxyphenyl)acetamide 3l with 7a according to the procedure described for SAPA 1a. Yield 76%; mp 104.2–106.3 °C. ESI-MS m/z 441.3 (M+H)⁺. HRMS (ESI) of C₂₃H₂₄N₂O₅S (M+H)⁺ calcd, 441.1479; found, 441.1483. ¹H NMR (400 MHz, DMSO-*d*₆) δ 9.29 (s, 1H), 8.00 (d, *J* = 7.7 Hz, 1H), 7.72 (d, *J* = 8.8 Hz, 2H), 7.59 (t, *J* = 5.8 Hz, 1H), 7.24 (t, *J* = 7.3 Hz, 2H), 7.20–7.02 (m, 7H), 6.91 (t, *J* = 7.5 Hz, 1H), 4.86 (s, 2H), 3.83 (s, 3H), 2.91 (q, *J* = 13.6, 7.2 Hz, 2H), 2.65 (t, *J* = 7.5 Hz, 2H). ¹³C NMR (101 MHz, DMSO-*d*₆) δ 166.0, 160.5, 149.5, 138.8, 132.9, 128.8, 128.5, 126.4, 125.1, 120.5, 115.2, 111.3, 67.1, 55.9, 44.2, 35.3. HPLC purity: *t*_R = 10.389, 100%.

4.2.1.19. 2-(4-(*N*-Phenethylsulfamoyl)phenoxy)-*N*-(*o*-tolyl)acetamide (SAPA 1r). SAPA 1r was prepared by the reaction of 2-chloro-*N*-(*o*-tolyl)acetamide 3m with 7a according to the procedure described for SAPA 1a. Yield 66%; mp 112.8–114.3 °C. ESI-MS m/z 425.2 (M+H)⁺. HRMS (ESI) of C₂₃H₂₄N₂O₄S (M+H)⁺ calcd, 425.1530; found, 425.1527. ¹H NMR (400 MHz, DMSO-*d*₆) δ 9.57 (s, 1H), 7.74 (d, *J* = 8.8 Hz, 2H), 7.59 (t, *J* = 5.8 Hz, 1H), 7.37 (d, *J* = 7.6 Hz, 1H), 7.25 (t, *J* = 7.3 Hz, 2H), 7.22–7.07 (m, 8H), 4.84 (s, 2H), 2.91 (q, *J* = 7.2 Hz, 2H), 2.66 (t, *J* = 7.5 Hz, 2H), 2.12 (s, 3H). ¹³C NMR (101 MHz, DMSO-*d*₆) δ 166.1, 160.6, 138.8, 135.5, 132.7, 132.3, 130.4, 128.7, 128.4, 126.3, 126.1, 125.8, 125.4, 115.2, 67.1, 44.2, 35.3, 17.7. HPLC purity: *t*_R = 7.623, 97.2%.

4.2.1.20. *N*-(2-Nitrophenyl)-2-(4-(*N*-phenethylsulfamoyl)phenoxy)acetamide (SAPA 1s). SAPA 1s was prepared by the reaction of 2-chloro-*N*-(2-nitrophenyl)acetamide 3n with 7a according to the procedure described for SAPA 1a. Yield 59%; mp 182.0–185.1 °C. ESI-MS m/z 456.2 (M+H)⁺. HRMS (ESI) of C₂₂H₂₁N₃O₆S (M+H)⁺ calcd, 456.1224; found, 456.1227. ¹H NMR (400 MHz, DMSO-*d*₆) δ 10.83 (s, 1H), 8.07 (dd, *J* = 8.3, 1.3 Hz, 2H), 7.78–7.72 (m, 3H), 7.60 (t, *J* = 5.5 Hz, 1H), 7.41–7.34 (m, 1H), 7.27–7.15 (m, 5H), 7.12 (d, *J* = 6.9 Hz, 2H), 4.87 (s, 2H), 2.91 (dd, *J* = 13.0, 7.2 Hz, 2H), 2.64 (t, *J* = 7.5 Hz, 2H). ¹³C NMR (101 MHz, DMSO-*d*₆) δ 166.6, 159.9, 140.3, 138.6, 134.8, 133.1, 131.4, 128.7, 128.6, 128.3, 126.2, 125.3, 125.2, 124.1, 115.1, 67.0, 44.0, 35.1. HPLC purity: *t*_R = 13.421, 98.0%.

4.2.1.21. *N*-(2-Cyanophenyl)-2-(4-(*N*-phenethylsulfamoyl)phenoxy)acetamide (SAPA 1t). SAPA 1t was prepared by the reaction of 2-chloro-*N*-(2-cyanophenyl)acetamide 3o with 7a according to the procedure described for SAPA 1a. Yield 36%; mp 169.4–172.4 °C. ESI-MS m/z 436.2 (M+H)⁺. HRMS (ESI) of C₂₃H₂₁N₃O₄S (M+H)⁺ calcd, 436.1326; found, 436.1321. ¹H NMR (400 MHz, DMSO-*d*₆) δ 10.44 (s, 1H), 7.83 (dd, *J* = 7.8, 1.1 Hz, 1H), 7.73 (d, *J* = 8.8 Hz, 2H), 7.71–7.67 (m, 1H), 7.62 (t, *J* = 6.8 Hz, 2H), 7.38 (dd, *J* = 11.8, 4.3 Hz, 1H), 7.24 (t, *J* = 7.3 Hz, 2H), 7.17 (d, *J* = 8.6 Hz, 3H), 7.15–7.11 (m, 2H), 4.90 (s, 2H), 2.91 (q, *J* = 7.2 Hz, 2H), 2.65 (t, *J* = 7.5 Hz, 2H). ¹³C NMR (101 MHz, DMSO-*d*₆) δ 166.8, 160.4, 139.3, 138.7, 133.9, 133.2, 132.8, 128.6, 128.3, 126.2, 125.7, 116.7, 115.1, 107.8, 66.8, 44.1, 35.2. HPLC purity: *t*_R = 6.016, 98.1%.

4.2.1.22. 2-(4-(*N*-Phenethylsulfamoyl)phenoxy)-*N*-(2-(trifluoromethoxy)phenyl)acetamide (SAPA 1u). SAPA 1u was prepared by the reaction of 2-chloro-*N*-(2-(trifluoromethoxy)phenyl)acetamide 3p with 7a according to the procedure described for SAPA 1a. Yield 55%; mp 124.3–126.6 °C. ESI-MS m/z 495.2 (M+H)⁺. HRMS (ESI) of C₂₃H₂₁F₃N₂O₅S (M+H)⁺ calcd, 495.1196; found, 495.1193. ¹H NMR (400 MHz, DMSO-*d*₆) δ 9.92 (s, 1H), 7.85 (dd, *J* = 8.0, 1.4 Hz, 1H), 7.71 (d, *J* = 8.9 Hz, 2H), 7.59 (t, *J* = 5.6 Hz, 1H), 7.44–7.38 (m, 1H), 7.36 (dd, *J* = 7.9, 1.4 Hz, 1H), 7.29 (dd, *J* = 7.8, 1.5 Hz, 1H), 7.27–7.21 (m, 2H), 7.17 (d, *J* = 7.2 Hz, 1H), 7.14–7.10 (m, 4H), 4.88 (s, 2H), 2.90 (q, *J* = 7.2 Hz,

2H), 2.65 (t, $J = 7.5$ Hz, 2H). ^{13}C NMR (101 MHz, DMSO- d_6) δ 166.5, 160.4, 140.4, 138.7, 132.7, 129.9, 128.6, 128.3, 127.7, 126.2, 125.5, 121.4, 118.8, 114.9, 66.8, 44.1, 35.2. HPLC purity: $t_R = 14.231$, 100%.

4.2.1.23. *N*-(3-Methoxyphenyl)-2-(4-(*N*-phenethylsulfamoyl)phenoxy)acetamide (SAPA 1v). SAPA 1v was prepared by the reaction of 2-chloro-*N*-(3-methoxyphenyl)acetamide **3q** with **7a** according to the procedure described for SAPA 1a. Yield 46%; mp 107.0–108.0 °C. ESI-MS m/z 441.3 ($\text{M}+\text{H}$) $^+$. HRMS (ESI) of $\text{C}_{23}\text{H}_{24}\text{N}_2\text{O}_5\text{S}$ ($\text{M}+\text{H}$) $^+$ calcd, 441.1479; found, 441.1479. ^1H NMR (400 MHz, DMSO- d_6) δ 10.13 (s, 1H), 7.71 (d, $J = 8.7$ Hz, 2H), 7.57 (s, 1H), 7.30 (s, 1H), 7.28–7.10 (m, 9H), 6.65 (d, $J = 7.9$ Hz, 1H), 4.79 (s, 2H), 3.70 (s, 3H), 2.91 (s, 2H), 2.65 (t, $J = 7.5$ Hz, 2H). ^{13}C NMR (151 MHz, DMSO- d_6) δ 166.4, 161.1, 160.0, 140.0, 139.2, 133.2, 130.1, 129.1, 128.8, 126.7, 115.5, 112.4, 109.7, 105.9, 67.5, 55.5, 44.6, 35.7. HPLC purity: $t_R = 8.100$, 98.9%.

4.2.1.24. *N*-(4-Fluoro-2-methoxyphenyl)-2-(4-(*N*-phenethylsulfamoyl)phenoxy)acetamide (SAPA 1w). SAPA 1w was prepared by the reaction of 2-chloro-*N*-(4-fluoro-2-methoxyphenyl)acetamide **3r** with **7a** according to the procedure described for SAPA 1a. Yield 74%; mp 161.3–163.5 °C. ESI-MS m/z 459.2 ($\text{M}+\text{H}$) $^+$. HRMS (ESI) of $\text{C}_{23}\text{H}_{23}\text{FN}_2\text{O}_5\text{S}$ ($\text{M}+\text{H}$) $^+$ calcd, 459.1384; found, 459.1386. ^1H NMR (400 MHz, DMSO- d_6) δ 9.33 (s, 1H), 7.92–7.84 (m, 1H), 7.72 (d, $J = 8.5$ Hz, 2H), 7.58 (s, 1H), 7.24 (t, $J = 7.2$ Hz, 2H), 7.15 (dd, $J = 17.4$, 8.9 Hz, 5H), 7.00 (d, $J = 10.9$ Hz, 1H), 6.74 (t, $J = 8.5$ Hz, 1H), 4.84 (s, 2H), 3.83 (s, 3H), 2.90 (s, 2H), 2.65 (t, $J = 7.5$ Hz, 2H). ^{13}C NMR (151 MHz, DMSO- d_6) δ 166.4, 160.9, 160.7, 159.1, 151.8, 139.2, 133.3, 129.1, 128.8, 126.7, 123.4, 123.2, 115.6, 106.6, 106.5, 100.4, 100.3, 67.5, 56.8, 44.6, 35.7. HPLC purity: $t_R = 10.451$, 99.4%.

4.2.2. The preparation of 4-(2-((4-chlorobenzyl)amino)-2-oxoethoxy)-*N*-substituted-benzamide (SAPA 1b,1c)

4.2.2.1. Methyl 4-hydroxybenzoate (9). To a solution of **8** (10.00 g, 72 mmol) in methanol (20 ml) was added SOCl_2 (6.8 ml) dropwise at 0 °C under N_2 . The reaction mixture was stirred at 70 °C for 2 h and then cooled to room temperature. After the organic solvent was evaporated, the residue was extracted by ethyl acetate, washed with brine and dried over Na_2SO_4 . After filtration and evaporation, **9** was obtained as white solid (10.00 g, yield 91%) and was used in next step without further purification. ESI-MS m/z 153.1 ($\text{M}+\text{H}$) $^+$.

4.2.2.2. Methyl 4-(2-((4-chlorobenzyl)amino)-2-oxoethoxy)benzoate (10). To a solution of **9** (3.49 g, 22.9 mmol) and **3a** (5.00 g, 22.9 mmol) in CH_3CN (100 ml) was added K_2CO_3 (6.32 g, 45.8 mmol). The reaction mixture was heated at 68 °C for 2 h and then cooled to ambient temperature. After the organic solvent was evaporated, the residual was diluted with ethyl acetate/water. The organic layer was washed with brine, dried over Na_2SO_4 and condensed. **10** was afforded as yellow solid (7.23 g, yield 94%) and used without further purification. ESI-MS m/z 334.1 ($\text{M}+\text{H}$) $^+$.

4.2.2.3. 4-(2-((4-Chlorobenzyl)amino)-2-oxoethoxy)benzoic acid (11). To a solution of **10** (4.00 g, 12 mmol) in THF (12 ml) and H_2O (12 ml) was added $\text{LiOH}\cdot\text{H}_2\text{O}$ (1.16 g, 48 mmol). The reaction mixture was stirred at 40 °C for 2 h and then the organic solvent was evaporated. The residue was poured into HCl (aq, 2 mol/L). The solid was filtered, washed with water and dried in vacuum. **11** was obtained as white solid (3.60 g, yield 94%); mp 214.1–216.5 °C. ESI-MS m/z 318.1 ($\text{M}-\text{H}$) $^-$. ^1H NMR (400 MHz, DMSO- d_6) δ 8.74 (s, 1H), 7.87 (d, $J = 8.9$ Hz, 2H), 7.34 (d,

$J = 8.6$ Hz, 2H), 7.24 (d, $J = 8.6$ Hz, 2H), 7.02 (d, $J = 8.9$ Hz, 2H), 4.61 (s, 2H), 4.32 (d, $J = 5.8$ Hz, 2H).

4.2.2.4. 4-(2-((4-Chlorobenzyl)amino)-2-oxoethoxy)-*N*-phenethylbenzamide (SAPA 1b). To a mixture of **11** (0.13 g, 0.41 mmol) and (3-(dimethylamino)propyl)ethylcarbodiimide hydrochloride (EDC, 94 mg, 0.49 mmol) in CH_2Cl_2 (10 ml) was added 1,2,3-benzotriazol-1-ol monohydrate (HOBt, 69 mg, 0.45 mmol). A clear solution was observed after stirring for 30 min, and **6a** (49 mg, 0.41 mmol) was added to the reaction solution, which was stirred at ambient temperature overnight (12 h). The reaction solution was washed with water and brine, dried over Na_2SO_4 and subjected to flash chromatograph eluting with ethyl acetate/heptanes (3:1) to provide **1b** as white solid (0.10 g, yield 58%); mp 203.0–204.5 °C. ESI-MS m/z 423.2 ($\text{M}+\text{H}$) $^+$. HRMS (ESI) of $\text{C}_{24}\text{H}_{23}\text{ClN}_2\text{O}_3$ ($\text{M}+\text{H}$) $^+$ calcd, 423.1470; found, 423.1475. ^1H NMR (400 MHz, DMSO- d_6) δ 8.72 (s, 1H), 8.44 (s, 1H), 7.79 (d, $J = 8.2$ Hz, 2H), 7.35 (d, $J = 7.9$ Hz, 2H), 7.31–7.15 (m, 7H), 7.00 (d, $J = 8.4$ Hz, 2H), 4.61 (s, 2H), 4.31 (d, $J = 5.5$ Hz, 2H), 3.45 (d, $J = 5.8$ Hz, 2H), 2.82 (t, $J = 6.8$ Hz, 2H). ^{13}C NMR (151 MHz, DMSO- d_6) δ 168.0, 166.0, 160.3, 140.1, 138.8, 131.8, 129.6, 129.3, 129.1, 128.8, 128.6, 128.0, 126.5, 114.7, 67.4, 41.7, 41.3, 35.7. HPLC purity: $t_R = 11.315$, 99.0%.

4.2.2.5. 4-(2-((4-Chlorobenzyl)amino)-2-oxoethoxy)-*N*-(pyridin-4-yl)benzamide (SAPA 1c). SAPA 1c was prepared by the reaction of **11** with pyridin-4-amine **6e** according to the procedure as described for SAPA 1b. To a solution of **1c** (0.40 g, 1.0 mmol) in dry ethyl acetate (10 ml) was added HCl (g)/ethyl acetate (1.2 ml, 1.5 mmol, $c = 1.25$ mol/L) dropwise at 0 °C. Then the solid was filtered and dried in vacuum. The hydrochloride of **1c** was given as white solid (0.34 g, yield 79%); mp 193.0–197.0 °C. ESI-MS m/z 396.1 ($\text{M}+\text{H}$) $^+$. HRMS (ESI) of $\text{C}_{21}\text{H}_{18}\text{ClN}_3\text{O}_3$ ($\text{M}+\text{H}$) $^+$ calcd, 396.1109; found, 396.1116. ^1H NMR (400 MHz, DMSO- d_6) δ 10.47 (s, 1H), 8.76 (s, 1H), 8.46 (s, 2H), 7.96 (d, $J = 8.4$ Hz, 2H), 7.78 (d, $J = 4.8$ Hz, 2H), 7.36 (d, $J = 7.9$ Hz, 2H), 7.27 (d, $J = 8.0$ Hz, 2H), 7.11 (d, $J = 8.4$ Hz, 2H), 4.66 (s, 2H), 4.32 (d, $J = 5.5$ Hz, 2H). ^{13}C NMR (151 MHz, DMSO- d_6) δ 167.9, 166.2, 161.2, 150.5, 146.8, 138.8, 131.9, 130.3, 129.6, 128.7, 127.3, 115.0, 114.5, 67.5, 41.7. HPLC purity: $t_R = 2.541$, 98.8%.

4.3. Biological evaluation

4.3.1. Materials

6-((*N*-(7-Nitrobenz-2-oxa-1,3-diazol-4-yl)amino)hexanoyl)-sphingosine (C6-NBD-Cer) and 1,2-dimyristoyl-*sn*-glycero-3-phosphocholine (DMPC) were purchased from Santa Cruz Inc (USA). D609, the public SMS inhibitor, was purchased from MedChem Express Inc. Milli-Q deionized water from a Millipore water purification system (Bedford, MA, USA) was used throughout the study. All other reagents were of analytical grade. Buffer 1 (0.25 M sucrose, 50 mM Tris-HCl, pH 7.4, 1 mM EDTA) was prepared for the storage of SMS1 overexpressing Hela cell lysate. Buffer 2 (100 mM HEPES, pH 7.4, 30 mM MnCl_2 , 3% BSA) was prepared for the assay of SMS1 inhibitory activities.

An Agilent 1260 HPLC system with a G1311B quaternary pump, a G1329B ALS and a G1321B FLD detector was used in our study. An Agilent C18 RP column (250 mm \times 4.6 mm, 5 μm) was employed in the chromatographic separations.

4.3.2. SMS1 overexpressed Hela cell lysate

Hela cells were purchased from the ATCC and maintained in DMEM high glucose medium with 10% fetal bovine serum at 37 °C in 5% CO_2 . Hela cells overexpressed SMS1 was established

by transfecting with pcDNA3.1 vector containing SMS1 and maintained in DMEM, 10% fetal bovine serum with G418 (final concentration 500 µg/mL) for every generation thereafter. Cells overexpressed SMS1 were then subcultured and siRNA for SMS2 were transfected when cells were 60% confluence. Three days after siRNA SMS2 treatment, cells were washed with PBS three times and suspended in SMS activity assay buffer (0.25 M sucrose, 50 mM Tris-HCl pH 7.4, 1 mM EDTA, 100 µg/ml phenylmethylsulfonyl fluoride, 1 µg/ml aprotinin and 1 µM leupeptin) after being scraped from dishes. SMS1 overexpressed Hela cells were homogenized by glass bead homogenizer. The cell lysates were centrifuged at 700 g for 10 min at 4 °C. The postnuclear supernatant was collected as the source of enzyme for determining the SMS1 inhibitory activities of SAPA derivatives.²⁸

4.3.3. SMS1 inhibitory activities assay in vitro

294 µl test mixture, which contained 28 µl SMS1 overexpressed Hela cell lysate (equivalent to 0.5 mg total protein) in buffer 1, 10 µl DMSO solution of the corresponding SAPA derivatives, 30 µl buffer 2 and 226 µl water, was pre-incubated at 37 °C for 30 min. Then 3 µl C6-NBD-Cer in DMSO (1.0 mM) and 3 µl DMPC in DMSO (40 mM) were added as substrates into the biological test system. Subsequently, the total 300 µl mixture was incubated at 37 °C for an additional 2.0 h. The test system was quenched by 600 µl ethanol and centrifuged at 10000 rpm for 10 min. The supernatant was collected and the amount of C6-NBD-Cer and C6-NBD-SM in the supernatant were quantified by a fluorescent HPLC-based analytic method.²⁷ 20 µl extracts from the supernatant were analyzed for the formation of C6-NBD-SM by HPLC using the reversed-phase C18 column and an isocratic elution with methanol/water/trifluoroacetic acid (89:11:0.1 (v/v)). The flow rate of the mobile phase was 1.0 mL/min. Detection was performed with a fluorescence spectrophotometer ($\lambda_{\text{excitation}} = 475 \text{ nm}$, $\lambda_{\text{emission}} = 525 \text{ nm}$). Assays were accomplished at least in triplicate. Statistical analysis was performed on Prism 5.02 (GraphPad Software, Inc.).

4.4. Molecular docking

The reported three-dimensional structure of human sphingomyelin synthase 1 was employed and loaded into the GOLD software suite (version 5.0, released by CCDC). Small molecules for docking studies were docked into the active site of hSMS1. The three-dimensional structures of substrate PC and SMS1 inhibitors including SAPA **1a**, **1b** and **D609** were constructed and energy optimized. Then the optimized structures of these molecules were selected as the docking ligands. The GA runs for each ligand were set 30 and therefore thirty binding poses were generated for each docked molecule. The scoring function in the docking process was set as GoldScore. The genetic algorithm (GA) search options were set as preset with 100,000 operations. The pose with the highest binding score of each docked ligand was selected out and studied for the interaction with hSMS1.

4.5. Point mutagenesis

All the methods were performed and modified as previous paper.¹⁷ Details are described as followed.

4.5.1. Plasmids

Expressing vector containing SMS1 was purchased from Open Biosystems (BC117782). SMS1 was subcloned into p3XFLAG-CMVTM-14 expression vector (Sigma) using restriction enzyme site EcoRI and SalI. All point mutations were created by Site mutagenesis QuikChange[®] II Site-Directed Mutagenesis Kit (Stratagene). Mutated plasmids were directly sequenced.

4.5.2. Cell culture and transfection

Hela cells were cultured in the 5% CO₂, 37 °C water bath with DMEM, 10% (v/v) FBS, 100 U/ml penicillin and streptomycin, and 2 mM glutamine. Plasmids were transfected into Hela cells with Lipofectamine[®] 2000 (Invitrogen).

4.5.3. Immunoprecipitation

Cells expressing SMS1-Flag were lysed with CelLytic[™] M buffer (Sigma). After cell debris were cleared at 8200 g for 10 min, supernatants were collected and blocked with 30 µl Protein A/G PLUS-Agarose Beads for 30 min. Beads were centrifuged 30 s at 8,200 g and supernatant was then incubated with 30 µl EZview[™] Red ANTI-FLAG M2 Affinity Gel (Sigma) for overnight.

4.5.4. Western blot

After immune precipitation, SDS PAGE loading buffer was added into ANTI-FLAG M2 Affinity Gel and the mixture was boiled at 95 °C for 5 min. Eluted protein was used, separated on the SDS page and then immunoblotted with an anti-Flag HRP (Sigma) for 1 h. Then protein was detected by the chemiluminescence method (Pierce).

4.5.5. SMS1 activity

After immune precipitation, ANTI-FLAG M2 Affinity Gel bound with SMS1-Flag were incubated with 50 mM Tris-HCl (pH 7.4), 25 mM KCl, C6-NBD-Ceramide (0.1 µg/µL), and phosphatidylcholine (0.01 µg/µL) at 37 °C for 1 h. Lipids were extracted by chloroform/methanol (2:1/v:v). Then lipids were separated on Thin Layer Chromatography Plates (Whatman) with CHCl₃/methanol/ammmoniac hydroxide (14:6:1).

Acknowledgments

We gratefully acknowledge the financial support from the Chinese National Natural Science Foundation (Grant No. 30973641), the Key Scientific and Technological Foundation of Shanghai Science and Technology Committee (Grant No. 11431920102), the 12th Graduate Innovation Foundation of Fudan University, and the open grant of the State Key Laboratory of Bio-organic and Natural Products Chemistry, CAS.

Supplementary data

Supplementary data associated with this article can be found, in the online version, at <http://dx.doi.org/10.1016/j.bmc.2015.07.060>.

References and notes

- Nilsson, Å.; Duan, R.-D. *J. Lipid Res.* **2006**, *47*, 154.
- Dougherty, R. M.; Galli, C.; Ferro-Luzzi, A.; Iacono, J. *Am. J. Clin. Nutr.* **1987**, *45*, 443.
- Bagdade, J. D.; Buchanan, W. E.; Kuusi, T.; Taskinen, M.-R. *Arterioscler. Thromb. Vasc. Biol.* **1990**, *10*, 232.
- Jiang, X.-C.; Paultre, F.; Pearson, T. A.; Reed, R. G.; Francis, C. K.; Lin, M.; Berglund, L.; Tall, A. R. *Arterioscler. Thromb. Vasc. Biol.* **2000**, *20*, 2614.
- Schlitt, A.; Blankenberg, S.; Yan, D.; von Gyzicki, H.; Buerke, M.; Werdan, K.; Bickel, C.; Lackner, K. J.; Meyer, J.; Rupprecht, H. J.; Jiang, X. C. *Nutr. Metab.* **2006**, *3*, 5.
- Li, Z.; Hailemariam, T. K.; Zhou, H.; Li, Y.; Duckworth, D. C.; Peake, D. A.; Zhang, Y.; Kuo, M.-S.; Cao, G.; Jiang, X.-C. *Biochim. Biophys. Acta (BBA)-Mol. Cell Biol. Lipids* **2007**, *1771*, 1186.
- Yeang, C.; Ding, T.; Chirico, W. J.; Jiang, X.-C. *Nutr. Metabol.* **2011**, *8*, 1.
- Allan, D.; Obradors, M. J. *Biochim. Biophys. Acta* **1999**, *8*, 277.
- Ding, T.; Li, Z.; Hailemariam, T.; Mukherjee, S.; Maxfield, F. R.; Wu, M.-P.; Jiang, X.-C. *J. Lipid Res.* **2008**, *49*, 376.
- Dong, J.; Liu, J.; Lou, B.; Li, Z.; Ye, X.; Wu, M.; Jiang, X.-C. *J. Lipid Res.* **2006**, *47*, 1307.
- Yan, N.; Ding, T.; Dong, J.; Li, Y.; Wu, M. *Lipids Health Dis.* **2011**, *10*, 46.
- Gowda, S.; Yeang, C.; Wadgaonkar, S.; Anjum, F.; Grinkina, N.; Cutaia, M.; Jiang, X.-C.; Wadgaonkar, R. *Am. J. Physiol.-Lung Cell. Mol. Physiol.* **2011**, *300*, L430.

13. Li, Z.; Fan, Y.; Liu, J.; Li, Y.; Huan, C.; Bui, H. H.; Kuo, M.-S.; Park, T.-S.; Cao, G.; Jiang, X.-C. *Arterioscler. Thromb. Vasc. Biol.* **2012**, 32, 1577.
14. Jiang, X.-C.; Yeang, C.; Li, Z.; Chakraborty, M.; Liu, J.; Zhang, H.; Fan, Y. *Clin. Lipidol.* **2009**, 4, 595.
15. Huitema, K.; van den Dikkenberg, J.; Brouwers, J. F.; Holthuis, J. C. *EMBO J.* **2004**, 23, 33.
16. Yamaoka, S.; Miyaji, M.; Kitano, T.; Umehara, H.; Okazaki, T. *J. Biol. Chem.* **2004**, 279, 18688.
17. Yeang, C.; Varshney, S.; Wang, R.; Zhang, Y.; Ye, D.; Jiang, X.-C. *Biochim. Biophys. Acta (BBA)-Mol. Cell Biol. Lipids* **2008**, 1781, 610.
18. Taniguchi, M.; Okazaki, T. *Biochim. Biophys. Acta (BBA)-Mol. Cell Biol. Lipids* **1841**, 2014, 692.
19. Zhang, Y.; Lin, F.; Deng, X.; Wang, R.; Ye, D. *Chin. J. Chem.* **2011**, 29, 1567.
20. Sauer, G.; Amtmann, E.; Melber, K.; Knapp, A.; Müller, K.; Hummel, K.; Scherm, A. *Proc. Natl. Acad. Sci.* **1984**, 81, 3263.
21. Gusain, A.; Hatcher, J. F.; Adibhatla, R. M.; Wesley, U. V.; Dempsey, R. J. *Mol. Neurobiol.* **2012**, 45, 455.
22. Meng, A.; Luberto, C.; Meier, P.; Bai, A.; Yang, X.; Hannun, Y. A.; Zhou, D. *Exp. Cell Res.* **2004**, 292, 385.
23. Bai, A.; Meier, G. P.; Wang, Y.; Luberto, C.; Hannun, Y. A.; Zhou, D. *J. Pharmacol. Exp. Ther.* **2004**, 309, 1051.
24. Zama, K.; Mitsutake, S.; Watanabe, K.; Okazaki, T.; Igarashi, Y. *Chem. Phys. Lipids* **2012**, 165, 760.
25. Deng, X.; Lin, F.; Zhang, Y.; Li, Y.; Zhou, L.; Lou, B.; Li, Y.; Dong, J.; Ding, T.; Jiang, X. *Eur. J. Med. Chem.* **2014**, 73, 1.
26. Lou, B.; Dong, J.; Li, Y.; Ding, T.; Bi, T.; Li, Y.; Deng, X.; Ye, D.; Jiang, X.-C. *PLoS ONE* **2014**, 9, 1.
27. Deng, X.; Sun, H.; Gao, X.; Gong, H.; Lu, W.; Chu, Y.; Zhou, L.; Ye, D. *Anal. Lett.* **2012**, 45, 1581.
28. Ding, T.; Kabir, I.; Li, Y.; Lou, C.; Yazdanyar, A.; Xu, J.; Dong, J.; Zhou, H.; Park, T.; Boutjdir, M. *J. Lipid Res.* **2015**, 56, 537.